Balancing Climate Change and Economic Development: the Case of China

Lin, Fan and Xie, Danyang

The Division of Emerging Interdisciplinary Areas, Academy of Interdisciplinary Studies, the Hong Kong University of Science and Technology, Thrust of Innovation, Policy and Entrepreneurship, Society Hub, The Hong Kong University of Science and Technology (Guangzhou)

2023

Balancing Climate Change and Economic Development: the Case of China

By Fan Lin and Danyang Xie *

We analyze China's economic growth and climate change relationship using a dynamic equilibrium model with regional disparity. Our simulation findings suggest that without intervention, China's temperatures could rise to $4.7°C$ *and* $3.4°C$ *in advanced and backward regions, respectively, by mid-next century. A social planner path could limit this rise to* $3.3°C$ *across both regions, yielding welfare benefits. However, if China adheres to the Paris Agreement's* $2°C$ *limit without exceptional low-carbon technology advancements, significant social welfare losses could occur.*

JEL: E27, E61, Q54

Keywords: Economic Development, Climate Change, China

* Lin: the Division of Emerging Interdisciplinary Areas, Academy of Interdisciplinary Studies, the Hong Kong University of Science and Technology, email: flinam@eonnct.ust.hk. Xie: Thrust of Innovation, Policy and Entrepreneurship, Society Hub, The Hong Kong University of Science and Technology (Guangzhou), and the Department of Economics, School of Business and Management, The Hong Kong University of Science and Technology, email: dxie@ust.hk. We provide an online appendix to include all technical details in https://dxie.people.ust.hk/online_appendix.pdf.

I. Introduction

Global temperatures have already risen by $1.1°C$ above pre-industrial levels, and with this change have come more frequent and severe weather events, underscoring the urgent need for action in the face of climate change. The Paris Agreement, with its goal to limit the increase in global temperature to below $2°C$, represents a collective effort to mitigate this crisis. The Sixth Assessment Report of the Intergovernmental Panel on Climate Change (IPCCAR6) starkly predicts a potential rise of $4.3°C$ if current policies and actions remain unchanged, a scenario far beyond the Agreement's thresholds. As the world's top emitter of carbon dioxide, China is at the forefront of this challenge, navigating the complex interplay between its rapid economic growth, heavy reliance on fossil fuels, and environmental commitments (Liu et al., 2021; Guan et al., 2016). In response, China has ratified the Paris Agreement and taken steps to decarbonize its economy, including implementing cap-and-trade pilot programs, investing in renewable energy sources, and exploring carbon capture, utilization, and storage (CCUS) technologies (Guan et al., 2016). However, the efficacy of such measures is debated, as previous implementations in different economies have shown limited success in reducing emissions effectively (Schneider and Kollmuss, 2015; Calel et al., 2021). This creates uncertainty about China's transition to a low-carbon economy and whether it can reconcile its developmental ambitions with the stringent targets set by the Paris Agreement.

In light of these challenges, our research indicates that the prevailing consensus may not hold firm without significant technological breakthroughs in carbon reduction. By employing a dynamic general equilibrium model, calibrated to account for the intricate relations between climate and economic factors across various regions and sectors, we analyze the optimal balance between environmental stewardship and economic growth. Our model recognizes the unique emission intensities and vulnerabilities to climate change that different areas and industries exhibit. It simulates the exchange of goods among these entities, capturing the economic ripple effects of carbon emissions that lead to increased temperatures and, consequently, reduced utility. Within this economic tapestry, the model envisions a social planner tasked with internalizing the cost of emissions and

orchestrating a balance between economic advancement and climate objectives. Through meticulous calibration using real-world data and IPCC projections, we simulate potential trajectories under different policy scenarios: a "laissez-faire" economy, a social planner solution, and strict adherence to the $2°C$ target of the Paris Agreement. Our findings are revealing: without a significant innovation in carbon reduction technology, the ambitious goals of the Paris Agreement may indeed prove to be more stringent than what might be deemed socially optimal. This insight underscores the need for a reassessment of climate targets in the context of technological capabilities and sets a stage for policy that supports and accelerates technological innovation in carbon reduction.

The quantitative results conclude that (1) the temperature rises of the advanced and backward regions would respectively exceed $4.7°C$ and $3.4°C$ in the "laissez-faire" economy[1], (2) the optimal path suggests temperature rises by around $3.3°C$ for both regions by the middle of next century with gains in welfare compared to the "laissez-faire" economy, and (3) to stick to the Paris Agreement goals, China would experience substantial losses in real GDP and welfare. Besides these findings, it is essential to note that the results and implications hinge on assumptions that excluded out-of-trend breakthroughs in low-carbon technologies. Technological breakthroughs in the future could significantly alter these findings, and this research calls for more attention to developing low-carbon technologies.

This research contributes to the literature mainly on three aspects: (1) building a dynamic general equilibrium model integrated with climate change model with regional disparity, (2) providing quantitative simulations of the Chinese economy and climate conditions in three scenarios based on a meticulous calibration and various data sources, and (3) proposing implementable tax-and-rebate policies to achieve the optimal path and the corresponding consequences quantitatively.

This research contributes to the macroeconomic literature integrating economic activities and climate change by harnessing multi-regional input-output tables in our model. The Nobel Prize laureate in 2018, Nordhaus pioneered the development of the (regional) dynamic integrated model of climate change

[1]Similarly, the temperature rises are $4°C$ (± 0.7) by the century end in the baseline projections of many sources (Nordhaus, 2017).

and economy (RICE/DICE) to establish a dynamic connection between climate change and economic development, aiming to identify the optimal path and policy implications (Nordhaus, 1994; Nordhaus and Yang, 1996)[2]. In the RICE/DICE model, carbon emissions from production contributes to temperature rises which in turn reduce productivity, and the studies are intended to find the optimal forward-looking decisions and investigate the outcomes under different solutions. In line with this approach, our model is aimed to explore the optimal path that maximizes the summation of discounted utility following the essence of a dynamic general equilibrium model. Distinctively, firstly, our model integrates the effects of climate change directly on utility with an infinite-time horizon, borrowing the insights of Acemoglu et al. (2012), which corresponds the thoughts that temperature rises directly deteriorate living quality. Secondly, our model identifies the relationships among various differentiated regions and sectors using the information of the multi-regional input-output (MRIO) table and climate observations at a disaggregate level. Thus, it characterizes the interrelations among diverse economic activities, and the varying vulnerability of regional climate to carbon emissions. Such modifications of regional disparity enhance its applicability, while requiring more decentralized data to support quantitative analysis and allowing for its use in a broader range of contexts.

Another noteworthy contribution of this research is the meticulous calibration. We employ robust and comprehensive strategies to determine parameters and exogenous variables, drawing upon real-world data from various sources, including input-output tables, regional and sector emissions, and climate information.

Additionally, this research is related to a large body of literature focused on policy implications for China to reduce carbon emissions. China started to consider the sustainable development and launched several low-carbon programs in the recent decade at small scales[3]. The difference-in-difference (DID) evalua-

[2]Nordhaus's work contributes significant insights to the literature. Nordhaus (1991) examines the historical context of greenhouse gases (GHGs) and their economic effects, Nordhaus (1992*b*) explains the DICE model with equations, Nordhaus (1992*a*) analyzes the ideal transition path for controlling greenhouse gases, Nordhaus (1994) offers a comprehensive overview of the economics of climate change, covering the scientific basis, economic impacts, and policy options, Nordhaus (2007*b*) highlights the significance of overall benefits in climate change mitigation policies, and Nordhaus (2011) analyzes social costs of carbon emissions bear by different regions.

[3]China initiated the carbon emission trading scheme (ETS) in 2013 in seven cities and expanded to eight sites. The national ETS was launched in 2017 and the first compliance cycle of the electricity generation industry was engaged in 2021.

tions of the pilot emission trading system find that it effectively reduces emissions in pilot cities and industries but incite them to outsource emissions to other places, constituting a problem of "carbon leakage" (Gao et al., 2020). The latest evaluation by Lyu et al. (2023) found Chinese low-carbon city pilots (LCCPs) policy is effective in reducing carbon emissions but with little declines in carbon emission per GDP and diminishing improvements over time. Besides China, the evaluations of the Clean Development Mechanism (CDM) and the Emissions Trading System (ETS) on the international societies are still debating over their effectiveness (Paulsson, 2009; Huang, Barker et al., 2008; Calel et al., 2021). Therefore, it is still ambiguous and controversial about the performance of existing policies and programs intended to mitigate climate change in China. The policymakers definitely need more solid analysis to expand the toolkit and further pursue low-carbon economy. The tax-and-rebate policy implications in this study represent a concrete application of Pigovian taxes to internalize the adverse effects of carbon emissions to the society. However, carbon taxes have not been adopted in China yet. This study not only offers comprehensive information for implementing tax-and-rebate policies for China, but also highlights the feasibility, efficiency, and potential consequences. Quantitative illustrations reveal the policy's capacity to substantially reduce carbon emissions, with only minor decreases in national GDP and overall improvements in social welfare. These insights are expected to equip policymakers with a valuable addition to their toolkit for combating climate change in China.

The remaining parts of this paper goes as follows: Section 2 presents the model and the policy implications, providing a solid foundation for the subsequent analysis. In Section 3, we elaborate our calibration strategies carefully as well as the performance of the calibrated model. Section 4 exhibits the dynamic results of the calibrated model and compares among different scenarios, shedding light on the potential impact of various policy interventions. Finally, in Section 5, we summarize the main findings of our research and highlight the implications for policy and future studies.

II. The Model

A. Benchmark Model: Laissez-faire Economy

The primary objective of the benchmark model is to provide a nuanced understanding of the economic system, elucidate the evolution of climate change, and capture their intricate interactions. In the benchmark model, the "laissez-faire" economy does not consider the negative impacts of climate change, while the losses are internalized in the "social planner" model. The entire economy is divided into two regions based on their wealth levels, namely an advanced region denoted as region A and a backward region as region B. Each region comprises two sectors that produce differentiated products, with one sector characterized by higher carbon emission intensity denoted as sector h, and the other sector with lower carbon emission intensity denoted as sector l. Indexes i and j represent regions while s and m label sectors.

In each period[4], the four production sectors utilize composite intermediates and labor to produce differentiated products through Cobb-Douglas production functions (equation II.1). By notations, Y_{is} refers to the amount of output of sector s in region i (or equivalently named as sector is), Z_{is}^h and Z_{is}^l are the high-emission and low-emission type composite intermediates used in sector is, A_{is} is the exogenous variable representing the total factor productivity (TFP), and L_{is} is the labor input. Parameters α_{is}^h and α_{is}^l controlling the factor shares are heterogeneous among sectors.

$$Y_{is} = A_{is}(Z_{is}^h)^{\alpha_{is}^h}(Z_{is}^l)^{\alpha_{is}^l}L_{is}^{1-\alpha_{is}^h-\alpha_{is}^l} \quad i \in \{A, B\}; s \in \{h, l\} \tag{II.1}$$

The composite intermediates consist of specific intermediates of the same type but different sources, through a constant elasticity of substitution (CES) aggregator (equation II.2). By notation, z_{is}^{Am} is the amount of specific intermediates from sector Am utilized in the production of sector is. The parameters ϵ controls the elasticity of substitution, and ω_{is}^{Am} and ω_{is}^{Bm} feature the weights between components such that $\omega_{is}^{Am} + \omega_{is}^{Bm} = 1$. Briefly speaking, (1) the capital letter Z and lower letter z differentiate whether the intermediates are composite or

[4] If not specified, time index t is omitted in the equations if all variables contain the same time index for simplicity.

specific; and (2) the subscript and superscript indicate the user and supplier respectively.

$$Z_{is}^{m} = \left[\omega_{is}^{Am}(z_{is}^{Am})^{\frac{\epsilon-1}{\epsilon}} + \omega_{is}^{Bm}(z_{is}^{Bm})^{\frac{\epsilon-1}{\epsilon}}\right]^{\frac{\epsilon}{\epsilon-1}} \quad i,j \in \{A,B\}; m \in \{h,l\} \tag{II.2}$$

We assume homogeneous people within the region. The populations of region A and region B are exogenous variables, denoted as L_{At} and L_{Bt} at period t, respectively. And each person supplies one unit of labor to the local labor market. Each one-person household faces utility maximization problem with an infinite time horizon, by deciding the amount of specific consumption of products from sector jm (denoted as c_i^{jm}) subject to the budget constraints (equation II.3). Because all the four sectors generate differentiated prodyucts, there are four product prices in this economy, i.e., p_{jm}.

$$\max_{c_i^{jm}(t)} \sum_{t=0}^{\infty} \rho^t U_{it} \quad \text{s.t.} \quad \sum_{m}\sum_{j} p_{jm}(t)c_i^{jm}(t) \leq W_i(t) \text{ for } t \in \mathbf{N} \tag{II.3}$$

The utility consists of two parts, i.e., $U_{it} = \ln(\Phi_{it}\mu_{it})$ where (1) Φ_{it} is the impacts of climate change, and (2) μ_{it} is the aggregate consumption through a series of CES aggregators (equation II.4 and II.5). The composition of composite consumption is similar to that of the composite intermediates. The parameter β is the constant elasticity of substitution between different types of composite consumption, the parameter σ is the elasticity of substitution between specific consumption, the parameters γ_h and γ_l control the preferences or weights such that $\gamma_h + \gamma_l = 1$, and the parameters η_i^{jm} are the weights such that $\eta_i^{Am} + \eta_i^{Bm} = 1$. Similar to the notations of intermediates, (1) the capital letter C and lower letter c discern the composite consumption and specific consumption and (2) the subscript indicates who consume the products and the superscript shows the product types.

$$\mu_i = \left(\gamma_h(C_i^h)^{\frac{\beta-1}{\beta}} + \gamma_l(C_i^l)^{\frac{\beta-1}{\beta}}\right)^{\frac{\beta}{\beta-1}} \tag{II.4}$$

$$C_i^m = \left[\eta_i^{Am}(c_i^{Am})^{\frac{\sigma-1}{\sigma}} + \eta_i^{Bm}(c_i^{Bm})^{\frac{\sigma-1}{\sigma}}\right]^{\frac{\sigma}{\sigma-1}} \tag{II.5}$$

Following the standard assumption for the complete and perfectly competitive market, each production sector is price-taker and faces a profit maximization problem by choosing the optimal specific intermediates and labor at the market

prices. Additionally, labor can not move across regions so that the wage cost is locally specified, i.e W_i. By substituting terms in the first order conditions, we can derive the equilibrium prices of composite intermediates Z_{is}^m (equation II.6) and of composite consumption C_i^m (equation II.7) such that $P_{is}^m Z_{is}^m = \sum_j p_{jm} z_{is}^{jm}$ and $P_i^m C_i^m = \sum_j p_{jm} c_i^{jm}$. Similarly, the capital letter P labels the composite prices while the lower letter p is the specific product price.

$$P_{is}^m = \left[(\omega_{is}^{Am})^\epsilon p_{Am}^{1-\epsilon} + (\omega_{is}^{Bm})^\epsilon p_{Bm}^{1-\epsilon}\right]^{\frac{1}{1-\epsilon}} \tag{II.6}$$

$$P_i^m = \left[(\eta_i^{Am})^\sigma p_{Am}^{1-\sigma} + (\eta_i^{Bm})^\sigma p_{Bm}^{1-\sigma}\right]^{\frac{1}{1-\sigma}} \tag{II.7}$$

In the literature, many studies introduce climate change impacts into economic models. The DICE model by Nordhaus (1994) shows that higher temperature negatively affects productivity. Others believe higher temperature negatively impacts utility and social welfare (Acemoglu et al., 2012). Following the latter insights, we define the impacts of climate change on region i at period t as a 0 to 1 discount factor to the aggregate consumption due to climate change, denoted as $\Phi_{it} \in [0, 1]$. The discount is a decreasing and concave function of the regional temperature rise above the pre-industrial era (denoted as $\Delta_{it} \geq 0$) such that $\Phi_{it} = \psi(\Delta_{it}) \in [0, 1]$ in equation II.8. The parameter D represents a dangerous temperature rise such that the impacts of climate change reach 100% degradation ($\psi(D) = 0$) and its marginal impacts are also unacceptable $\lim_{\Delta \to D^-} \frac{d\psi(\Delta)}{d\Delta} = -\infty$. For the temperature rise greater than the dangerous level ($\Delta_{it} > D$), the climate change discount factor keeps zero. The parameter $\lambda \in (0, 1)$ controls the concavity. The concavity means that as the temperature rises, the negative marginal effects enlarge on the discount due to climate change, indicating a more and more undesirable situation.

$$\psi(\Delta_{it}) = \begin{cases} \frac{(D-\Delta_{it})^\lambda - \lambda D^{\lambda-1}(D-\Delta_{it})}{(1-\lambda)D^\lambda} & , \Delta_{it} \in [0, D] \\ 0 & , \Delta_{it} > D \end{cases} \tag{II.8}$$

It is common sense that greenhouse gas (GHGs) emissions play a vital role in climate change, most of which are carbon dioxide (CO_2) induced by the usage of fossil fuels. The model hinges on this fact and assumes the carbon emissions of the region i is E_{it} in equation II.9, where the exogenous variable $\xi_{is}(t)$ are

the real emission factor. By their names, the high-emission sector (h) generates higher carbon emissions compared to the low-emission sector (l) in terms of the nominal emission intensity such that $\frac{\xi_{ih}(t)}{p_{ih}(t)} >> \frac{\xi_{il}(t)}{p_{il}(t)}$.

$$E_{it} = \xi_{ih}(t)Y_{ih}(t) + \xi_{il}(t)Y_{il}(t) \tag{II.9}$$

We define the regional atmospheric CO_2 concentration as Q_{it}. The temperature rise is an increasing function of atmospheric CO_2 concentration such that $\Delta_{it} = T(Q_{it})$ (equation II.10). In contrast to the DICE model and the work by Acemoglu et al. (2012), which assumes the doubling of atmospheric CO_2 concentration leads to a fixed temperature rise[5], we propose a more general form to capture the non-linear relationship between temperature and atmospheric CO_2 concentration, highlighting the importance of observed data. As the global atmospheric CO_2 concentration was around 280 parts per million (ppm) in pre-industrial level (GISTEMP, 2022), our analysis suggests $T(280) = 0$. In line with climate change impact in equation II.8, We define $\bar{Q} \triangleq 280[(\frac{D}{a})^{\frac{1}{b}} + 1]$ at which the temperature rise reaches the dangerous level ($T(\bar{Q}) = D$).

$$T(Q_{it}) = a\big(Q_{it}/280 - 1\big)^b \tag{II.10}$$

Thus, the relationship is built between the discount due to climate change Φ_{it} and the excessive atmospheric CO_2 concentration ($Q_{it}-280$), denoted as $\Phi_{it} = \phi(Q_{it})$ with $\phi = \psi \circ T$. The law of motion in equation II.A explains the relationship between E_{it} and $(Q_{it} - 280)$, with Q_{A0} and Q_{B0} given as parameters. The law of motion tells that the next period's CO_2 concentration consists of two parts: (1) remaining CO_2 concentration in the atmosphere after a natural absorption rate δ_i, and (2) carbon emissions E_{it} generate CO_2 particles in the atmosphere in a power relation ($G_i E_{it}^{\kappa_i}$). The parameters G_i and κ_i are positive, characterizing how carbon emissions transform into atmospheric CO_2 concentration for the next period. The region-related parameters characterize the regional disparity in the natural absorption rates (δ_i) and the capacity of carbon emission

[5]According to the IPCC, the climate sensitivity parameter measures the temperature change response to the doubling of CO_2 concentration, which is not fixed as temperature rise changes. The IPCC 5th Assessment Report in 2013 estimated that a doubling of CO2 concentration from 280 to 560 would likely result in a long-term warming of about $1.5°C$ to $4.5°C$, and the range became $2°C$ to $4°C$ with a best estimate of about $3°C$ in their 6th report in 2021.

transforming into atmospheric concentration (G_i and κ_i) due to the differences in environments and climate systems. Besides connecting carbon emissions and excessive atmospheric CO_2 concentration, these equations also illustrate the law of motion for the state variables Q_{it+1} in the dynamic economic system.

$$Q_{it+1} - 280 = (1 - \delta_i)(Q_{it} - 280) + G_i E_{it}^{\kappa_i} \tag{II.11}$$

In the benchmark model, carbon emissions are characterized by an externality, with no information available to anyone regarding the impacts of climate change. Production sectors do not consider carbon emissions in their decisions, and households are unaware of the negative consequences of climate change or the evolution of CO_2 concentration (Q_{it}) over time. The benchmark model equilibrium is established as a laissez-faire economy. For a given period t, a specific set of product prices $p_{is}(t)$ and labor wages $W_i(t)$ define the market equilibrium, such that the distribution of specific intermediates, labor, and consumption satisfy: (1) market clearing conditions (the four differentiated products are clear in equation II.12 and the local labor market is clear in equation II.13), (2) maximization of profits by each production sector, and (3) households' utility maximization. The equilibrium prices and wages are defined as the prices and incomes that prevail in the market, while the equilibrium distribution of products is defined as the distribution of products that occurs under the market equilibrium.

$$Y_{jm}(t) = \sum_i \sum_s z_{is}^{jm}(t) + \sum_i L_{it} c_i^{jm}(t) \text{ for } j \in \{A, B\}, m \in \{h, l\} \tag{II.12}$$

$$L_{it} = \sum_s L_{is}(t) \text{ for } i \in \{A, B\} \tag{II.13}$$

According to the first order conditions[6], the equilibrium outcomes in the benchmark model are independent of climate change and carbon emissions, as the model assumes that no entity possesses any information about climate change, all agents treat it as an exogenous factor, and all activities are geared toward maximizing economic benefits. In light of the atmospheric CO_2 concentration's law of motion (equation), it is possible to approach and even exceed $\bar{Q}$. In

[6]For details of equations, please refer to our online appendix.

such a case, the impacts of climate change become so severe that consumption becomes nearly meaningless to people ($\Phi_{it} \to 0$ and even $\Phi_{it} = 0$). Since the calibration process is not designed to prevent catastrophes, it is possible[7] that the benchmark model will generate results with $Q_{it} > \bar{Q}$. Although all agents succeed in maximizing their interests, the lack of consideration of climate change can harm the entire economy in the long run. The benchmark model serves as a warning and emphasizes the importance of actively addressing climate change, intervening in the market, and mitigating or eliminating the negative externality of carbon emissions.

The undesirable implications of the benchmark model are not unique to this study. The "laissez-faire" market results in a disastrous environment in a very close study by Acemoglu et al. (2012). From the model perspective, such a equilibrium fails to deal with climate change because carbon emissions generated by the production processes have a negative externality on households.

B. The Social Planner Model

Our analysis reveals that a laissez-faire economy fails to strike a balance between economic development and climate change, posing a significant catastrophe risk. This is primarily due to the assumption that no entity possesses any information about climate change and treats it as an exogenous factor. In order to address this issue and explore the optimal path for balancing economic development and climate change, we propose a model that introduces a social planner. Our analysis of this model highlights essential policy implications for achieving the optimal path.

Consider a social planner who aims to maximize the present value of total social utility with an infinite time horizon by distributing resources among regions and sectors subject to the product constraint and the labor constraint (from equation II.14 to equation II.16). The control variables of the social planner include all control variables in the benchmark model, i.e. $\mathbf{CV} = \{z_{is}^{jm}(t), L_{is}(t), c_i^{jm}(t) | s, m \in \{h, l\}, i, j \in \{A, B\} \text{ and } t \in \mathbf{N}\}$. As a very simple aggregation of the present values of the two regions' total utility, the social planner takes the weighted average of the two regions with the weight for region A's utility present value as $\theta_A = \theta$

[7]Indeed, the calibrated model results demonstrate that such severe catastrophes are prevented in the benchmark model, with details in Section 4.

and the weight for region B as $\theta_B = 1 - \theta$.

$$\max_{\mathbf{CV}} \quad \sum_{t=0}^{\infty} \rho^t \left(\theta_A L_{At} \ln\left(\Phi_{At}\mu_{At}\right) + \theta_B L_{Bt} \ln\left(\Phi_{Bt}\mu_{Bt}\right)\right) \tag{II.14}$$

$$\text{s.t. } \forall j, m, t \quad \sum_i \sum_s z_{is}^{jm}(t) + \sum_i c_i^{jm}(t) L_{it} \leq Y_{jm}(t) \tag{II.15}$$

$$\forall i, t \quad L_{ih}(t) + L_{il}(t) \leq L_{it} \tag{II.16}$$

Different from the benchmark model, the social planner knows all the information about climate change, including how it affects utility and how carbon emissions contribute to higher atmospheric CO_2 concentration over time. The social planner faces the constraints for the state variables Q_{it+1} for the two regions (equation II.17).

$$\forall i, t \quad Q_{it+1} - 280 = (1 - \delta_i)(Q_{it} - 280) + G_i E_{it}^{\kappa_i} \tag{II.17}$$

Denote Lagrangian multipliers to the product constraint II.15, the labor constraint II.16, and the motion of state variables Q_{it} II.17 as $\gamma_{jm}(t)$, $\gamma_{iL}(t)$ and w_{it}, respectively. They are the shadow prices of product jm, the labor of region i, and the state variable Q_{it+1}. Inada conditions of the production function, utility function, and climate change discount factor ($\phi(Q_{it})$) suggest that these multipliers are all strictly non-zero. Moreover, as $\lim_{Q \to \bar{Q}} \frac{d\phi(Q)}{dQ} = -\infty$, the social planner's optimal solution must prevent the situation. Henceforth, we can derive first-order conditions and Euler equations easily[8].

$$\tilde{\gamma}_{is}(t) = \gamma_{is}(t) + w_{it}\kappa_i G_i E_{it}^{\kappa_i - 1} \xi_{is}(t) \quad i \in A, B; s \in h, l \tag{II.18}$$

Define the carbon-deducted shadow prices of product is as its shadow price plus the negative impacts due to carbon emissions, denoted as $\tilde{\gamma}_{is}(t)$ in equation II.18. And we can rewrite the first order conditions for intermediates and labor inputs in equations II.19 below. They indicate that the climate-friendly price of the marginal product of factors should equal their shadow prices in the optimal solution.

$$\tilde{\gamma}_{is}(t) \frac{\partial Y_{is}(t)}{\partial z_{is}^{jm}(t)} = \gamma_{jm}(t) \quad ; \quad \tilde{\gamma}_{is}(t) \frac{\partial Y_{is}(t)}{\partial L_{is}(t)} = \frac{\gamma_{iL}(t)}{\gamma_i(t)} \tag{II.19}$$

[8]For details, please refer to our online appendix.

To investigate the optimal path to the optimization problem with an infinite time horizon, we need to find a steady state. For the time-relevant exogenous variables $\{A_{is}(t), \xi_{is}(t), L_{it}\}$, we parameterize their growth based on the logistic growth model such that they are convergent over time[9]. In terms of quantitative results, we assume these time-variant exogenous variables are fixed at their steady-state values when $t \geq ssT \triangleq 100$. And the economy gradually approaches its steady state where all variables are fixed at the market equilibrium.

Indicated by the necessary conditions for the optimal solution to the social planner model, a social planner is feasible to deal with the negative externality of carbon emissions on economic development by identifying the negative impacts of carbon emissions (equation II.18) and deducting it from the shadow value (equation II.19). The social planner model suggest policies of proportional production taxes and lump-sum rebates to internalize the social cost of carbon emissions. Specifically, the tax rate is $(\gamma_{is} - \tilde{\gamma}_{is})$ for production sector is on their sales. The taxes from the four sectors should be collected by the social planner and transferred to households of the two regions as lump-sum rebates (lump-sum taxes if negative). Because the social planner does not face the constraint that the rebate payment should equal tax revenue within the same region, we can only claim that the total lump-sum rebates of two regions equal the total tax revenues (equation II.20). With these policies, the market equilibrium can constitute the same outcomes as if there were a social planner.

$$\begin{aligned}(\overbrace{\sum_j \sum_m \gamma_{jm} L_{At} c_A^{jm} - \gamma_{AL} L_{At}}^{\textit{rebate to region A}}) + (\overbrace{\sum_j \sum_m \gamma_{jm} L_{Bt} c_B^{jm} - \gamma_{BL} L_{Bt}}^{\textit{rebate to region B}}) \\ = (\underbrace{\sum_s (\gamma_{As} - \tilde{\gamma}_{As}) Y_{As}}_{\textit{tax revenue from region A}}) + (\underbrace{\sum_s (\gamma_{Bs} - \tilde{\gamma}_{Bs}) Y_{Bs}}_{\textit{tax revenue from region B}})\end{aligned} \tag{II.20}$$

As the social planner has a full capacity to control all resources and full information about climate change, her strategy must achieve Pareto improvements. However, a social planner does not always provide a Pareto improvement to the benchmark across regions. The households in the two regions may not agree with the solution the social planner offers, i.e., the participation conditions are

[9]For details, please refer to the Section 3.

not satisfied. Because the model defines the total social utility as the weighted average of the household's utility of the two regions, the weight θ is crucial to achieve Pareto improvement or not for the social planner[10]. Nonetheless, she can designate the proper regional welfare weight θ to achieve Pareto improvement.

III. The Calibration

Data Processing. — The PRC Bureau of Statistics publishes *Chinese Regional Input-Output Table* for the years 2012, 2015, and 2017, which collects and adjusts the input-output table by 2-digit industries of 31 provincial-level areas in mainland China. Combined with the national input-output tables in corresponding years, the study by Zheng et al. (2020) applies a series of data processing methods and reports the multi-regional input-output (MRIO) tables for the years 2012 and 2015. They extended the data into the year 2017, and the data was released in the Carbon Emission Accounts & Datasets (CEADs).

Because our model only includes two regions and two sectors in a closed economy, we need to aggregate the MRIO table entries into a two-region and two-sector input-output table. By definition, region A is an advanced region, while region B is backward. Based on geographic proximity and topological characteristics, provinces of mainland China are divided into eight parts: northwest, north, northeast, central coast, central, southwest, south coast, and Beijing & Tianjin(BJTJ) area. China's economic characteristics show a noticeable pattern that the central coast, south coast, and BJTJ area are the more developed region[11]. Consequently, region A consists of the three developed parts (8 provinces in total), and region B takes the others (see Fig. III.1).

As for aggregating industries into two sectors, i.e., one high-emission sector(h) and one low-emission(l), carbon emission intensities concerning outputs are the criterion, i.e., emission of CO_2 per nominal output[12]. The platform CEADs provides provincial carbon emission inventory data by Intergovernmental Panel

[10] Unlike the Negishi weights adopted in the RICE model intended to constitute a market equilibrium where each region has zero excessive demands from the scope of international trade balances (Nordhaus and Yang, 1996), the weights in our model make the social planner achieve Pareto improvements for both regions so that both regions will accept her social plan.

[11] E.g., these areas take up 27.7% population and 40.9% GDP in 2022 according to the Chinese National Bureau of Statistics.

[12] In some contexts, the denominator is value-added or GDP. Because the model assumes emissions are generated through the production of outputs, the denominator here is output value

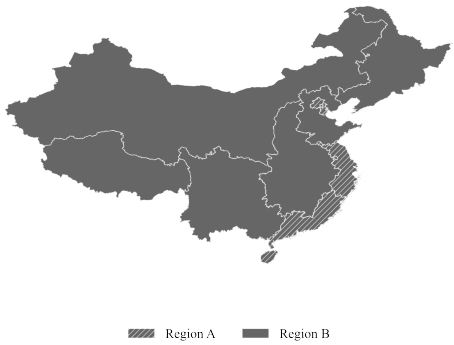

Figure III.1. : Division of mainland China in region A and region B

on Climate Change (IPCC) sectoral emissions from 1997 to 2019 (Guan et al., 2021; Shan et al., 2020, 2018, 2016). However, the IPCC sectors differ from the 42 industries in the MRIO table. We consolidate the classification based on 2-digit economic activities[13]. The definition of sector h and sector l is determined based on the carbon intensity distribution in the baseline year 2012. According to the computation, the top four industries have carbon intensities that exceed the national average of 56.6 grams of carbon emissions per CNY output in 2012, while the remaining industries have carbon intensities that fall below the national average, with a significant drop in intensity observed between the fourth and fifth industries [14]. Based on these observations, it is reasonable to classify the top four industries as the h sector. By names, sector h includes industries: (i) production and supply of electricity and heat, (ii) non-metallic mineral products, (iii) smelting and rolling of metals, and (iv) transportation, storage, and postal services. Statistically, the sector h accounts for 83.3% carbon emissions but only contributes 16.7% output to the economy (current GDP accounts for around 12.5%). To avoid the sensitivity of baseline year selection, the patterns of intensities in 2015 and 2017 are almost identical. Therefore, the definition of sectors h and l is robust to the baseline year.

Lastly, to consolidate the data with the assumption of a closed economy, we remove imports and exports and reallocate net exports to consumption expenditure with the same fraction between regions A and B while balance the regional

[13]Table A1 and A2 in the online appendix show how the IPCC sectors are merged into the 2-digit economics activity classification categories

[14]For visualization, see Figure A1 in the online appendix.

final uses and the value-added. The processed MRIO table meets the model requirements and shows no substantial differences from the raw data[15]. Henceforth, the MRIO table henceforth refers to the one after processing, which has a two-region and two-sector structure and includes no international trade.

FACTOR SHARES α_{is}^{m} AND POPULATION. — As the model implies, α_{is}^{m} is the share of the m-type composite intermediate used by sector is in its output value. Because we regard the year 2012 as the baseline for the calibration, the values of α_{is}^{m} are directly calculated[16] based on the MRIO table in 2012. Table III.1 reports the results.

Table III.1—: The calibration results of α_{is}^{m}

i	s	m	Value	i	s	m	Value
A	h	h	0.406	A	h	l	0.324
A	l	h	0.124	A	l	l	0.512
B	h	h	0.324	B	h	l	0.394
B	l	h	0.120	B	l	l	0.500

Note: Intuitively, for the total population and the population share of region A respectively, K^{L} and K^{LA} are the convergent maximum values, P_0^{L} and P_0^{LA} are the values at the baseline year 2012 ($t = 0$), and r^{L} and r^{LA} control the "S" shape.

To parameterize the exogenous variables of regional populations, especially its future pattern, we adopt Pearl-Verhulst logistic growth model (equations III.1 and III.2), assuming that population of each region follows a "S" shape pattern and converges to a certain level over time. We define the following structure mainly because the observations of total population and the share of region A exhibit clear logistic growth pattern.

$$L_t = f^{L}(t) \triangleq \frac{K_L P_L}{P_L + (K_L - P_L)e^{-r_L t}} \tag{III.1}$$

$$L_{At} = f^{LA}(t) \triangleq \frac{K_L^A P_L^A}{P_L^A + (K_L^A - P_L^A)e^{-r_L^A t}} \tag{III.2}$$

To determine these parameters, we collect regional population (1980 to 2021) from Chinese National Bureau of Statistics and apply the non-linear least square estimation. Table III.2 presents the parameter results[17].

[15] For details, please refer to Fig. A2 and Fig. A3.
[16] The results do not differ substantially if we turn to use the data in 2015 or 2017, which supports its robustness to the selection of baseline year.
[17] Fig. A4 in the online appendix exhibits the fitness.

Table III.2—: The calibration results of population parameters

Parameter	K_L	r_L	P_L	K_L^A	r_L^A	P_L^A
Value	1504.7	0.051	981.5	0.364	0.035	0.223

FIXED PARAMETERS ρ, ϵ AND σ. — The discount rate's value characterizes the utility's importance in the future, and we set the discount rate as $\rho = 0.98$. The calibration for the elasticity of substitution refers to the literature. It is intuitive to affirm that $\epsilon > 1$ and $\sigma > 1$ because the products are (gross) substitutes. For example, if the electricity generated from region A becomes more expensive, the household expenditure or the production factor input on electricity shifts to region B. Although the two parameters describe the elasticity in production and consumption, they both stipulate the elasticity of substitution between substitutes. Thus, it is grounded to give the two parameters the same value without losing the model generality. This study uses $\epsilon = 3$ and $\sigma = 3$ as the benchmark. In detail, the elasticity of substitution among varieties is estimated in the global trade literature (Broda and Weinstein, 2006), which becomes a very important reference for studies to determine the value of elasticity of substitution[18].

INITIAL TFPS $A_{is}(0)$ AND WEIGHTS ω_{is}^{jm} AND η_i^{jm}. — The calibrated model is supposed to derive the equilibrium of the benchmark model in the baseline year 2012 such that the shares of specific products in both production and consumption structure all match the MRIO data[19]. Such a strategy is intended to exploit all information from the MRIO table to feature the relationship among economic activities.

However, the MRIO structure information is not enough to determine these parameters due to the issue of redundant equations[20]. We turn to utilize price information to fix it. The work by Brandt and Holz (2006) provides the current cost of the joint basket in 1990 composition per capita and population by provinces of China. Following the classification of the region A and the region B, we calculate the current cost of the basket for two regions in the baseline year, denoted as $PC_A = 2.324$ and $PC_B = 2.018$ (thousand *yuan* CNY). Define the

[18]For the model performance with different parameter values, please refer to the robustness check D in the online appendix.
[19]If not specified, all notations refer to the period index at the year 2012 by default in this part.
[20]See B.B2 in our online appendix for details.

price of regional aggregate consumption as P_i such that $P_i\mu_i = \sum_j \sum_m p_{jm} c_i^{jm}$, and we obtain equation III.3 based on equation II.7. The calibration requires that the prices in the model should equal the cost of the basket, i.e., $P_i = PC_i$. Therefore, one unit of aggregate consumption μ_{it} can be interpreted as the number of joint baskets in 1990 composition.

$$P_i = \left(\gamma_h^{\beta}(P_i^h)^{1-\beta} + \gamma_l^{\beta}(P_i^l)^{1-\beta}\right)^{\frac{1}{1-\beta}} \tag{III.3}$$

The calibration results are presented in Table III.3, where the results of ω_{is}^{Bm} and η_i^{Bm} are omitted because it is assumed that $\omega_{is}^{Am} + \omega_{is}^{Bm} = 1$ and $\eta_i^{Am} + \eta_i^{Bm} = 1$. In conclusion, the calibrated benchmark model constitutes the market equilibrium in year 2012 such that: (1) the nominal value of specific intermediate match the data ($p_{jm} z_{is}^{jm}$); (2) the expenditures on specific consumption equal the data, i.e., $p_{jm} c_i^{jm}$; (3) incomes of households equal the value-added data (W_i); and (4) the output value of each sector equals the data ($p_{is} Y_{is}$).

Table III.3—: The calibration results of ω_{is}^{Am}, η_i^{Am} and $A_{is}(0)$

$A_{Ah}(0)$	228.624	$A_{Al}(0)$	7.069	$A_{Bh}(0)$	190.988	$A_{Bl}(0)$	9.533
ω_{Ah}^{Ah}	0.574	ω_{Ah}^{Al}	0.687	ω_{Al}^{Ah}	0.542	ω_{Al}^{Al}	0.745
ω_{Bh}^{Ah}	0.215	ω_{Bh}^{Al}	0.395	ω_{Bl}^{Ah}	0.222	ω_{Bl}^{Al}	0.387
η_{Ah}^{A}	0.608	η_{Al}^{A}	0.752	η_{Bh}^{A}	0.243	η_{Bl}^{A}	0.465

Note: As $\omega_{is}^{Am} + \omega_{is}^{Bm} = 1$ and $\eta_i^{Am} + \eta_i^{Bm} = 1$, this table only presents one half of these parameters. The TFP levels are not comparable because all products are differentiated. We need to rely on variables like nominal output per labor and labor wages to compare the productivity levels by regions and sectors.

Utility function parameters γ_s and β. — These parameters control households' preference between the two types of composite consumption products in the demand system (see equation B9). The study applies the nonlinear least square estimation w.r.t. equation III.4 to determine the parameters. As the sum of value-added shares of the two types is one, the covariance matrix of the error term in the demand system is singular. Therefore, we can conduct the estimation only using the share of sector h, which avoids problems with multi-equation estimation. Remarkably, we do not rely on consumption survey data for the estimation because the model does not include investment, and all consumption should equal value-added. Meanwhile, as the household utility function does

not differ across regions, we can exploit the national data for the estimation.

$$\text{(III.4)} \qquad \text{Value-added Share of Sector } h = \frac{\gamma_h^{\beta} P_{ht}^{1-\beta}}{\gamma_h^{\beta} P_{ht}^{1-\beta} + \gamma_l^{\beta} P_{lt}^{1-\beta}} + \text{Error term}$$

Because of the definitions for sectors h and l, we need to modify the value-added data in proper category. We utilize two sources of data to synthesize the value-added data by sectors h and l[21]: the Chinese National Bureau of Statistics and the Groningen Growth and Development Centre (GGDC) (Inklaar and Timmer, 2014).

Table III.4—: The calibration results of γ_h and β

Parameter	γ_h	β
Value	0.557***	0.0527***
	(0.0388)	(0.0106)

Note:

The standard deviation of the robust estimation is reported in the bracket.

The significance level works for the Leave-One-Out Cross-Validation (LOOCV). *** Significant at the 1 percent level. ** Significant at the 5 percent level. * Significant at the 10 percent level.

Given the limited number of annual observations, the results may suffer from outliers. To improve the accuracy of parameters, we conduct the Leave-One-Out Cross-Validation (LOOCV) for robustness check and summarize the results in Table III.4. The result $\beta \in (0, 1)$ shows that different composite products are (gross) complements in consumption.

TFPs $A_{is}(t)$. — Following the setting of convergent productivity parameters in the DICE model, the growth rates of A_{is} diminish with a fixed rate consistently over time. The equations III.5 and III.6 show the dynamic motion of $A_{is}(t)$ and the dynamic of growth rates, respectively, where $s \in \{h, l\}$ and $t \in \mathbf{N}$. To reduce the number of undetermined parameters, it is further assumed that (1) the growth rates for each period differ in sectors; and (2) the growth rates of all TFPs are within 0.1 percent right at $t = ssT = 100$, i.e., $\max\{g_h(100), g_l(100)\} = 0.1$ percent. Therefore, there are only two parameters to determine, $g_h(0)$ and $g_l(0)$, with $\delta = 1 - \left(\frac{0.1\%}{\max\{g_h(0), g_l(0)\}}\right)^{0.01}$ determined automatically.

$$\text{(III.5)} \qquad A_{is}(t+1) = (1 + g_s(t))A_{is}(t)$$

$$\text{(III.6)} \qquad g_s(t+1) = g_s(t)(1 - \delta)$$

[21] For details of the synthesis process, please see C.C1 in our online appendix.

The calibration targets are the value-added at the 2012 fixed price by region, which can be easily obtained from the Chinese National Bureau of Statistics. Because the model does not include physical capital, the summation of regional household incomes refers to the value-added in real data. The calibration results of $g_h(0)$ and $g_l(0)$ should constitute the regional household incomes in the DGE results that share a very similar pattern with the value-added data in the period (year 1992 to 2021, or equivalently $t \in [-20, 9]$). Specifically, the optimal values of parameters result in the minimized summation of residuals of the two sequences between value-added data and regional summation of household income. Using a grid search method such that $g_h(0) \in [3\%, 5\%]$ and $g_h(0) \in [2\%, 4\%]$ with 0.2% increments, we find the optimal solution is $g_h(0) = 0.036$, $g_l(0) = 0.026$ and $\delta = 0.0352$. Consequently, the calibration performs well as the results exhibit little differences between the regional household income predicted by the model and observations of regional value added (see Fig. A5 for visual compare).

Performance of the Calibrated Model. — The benchmark model has been solved given the determined economic parameters, as climate change does not change economic activities. We assess the performance of the calibrated model by evaluating its ability to predict non-target data. The data for the performance evaluation includes shares of jm intermediates in m composite intermediates $(\frac{p_{jm} z_{is}^{Am}}{P_{is}^{m} Z_{is}^{m}})$ and shares of jm consumption in m composite consumption $(\frac{p_{jm} c_{im}^{A}}{P_{im} C_{im}})$, where $i \in \{A, B\}$, $s, m \in \{h, l\}$, and j takes A by default but If takes B if the share of A is greater than 0.5.

In conclusion, denote non-targets for the performance evaluation as Obs_n with n indexes the items and denote the corresponding model results as Model_n. Statistically, the OLS regression $\text{Obs}_n = \text{CoefModel}_n + \epsilon_n$ shows that $\text{Coef} = 1$ falls into the 95 percent confidence interval[22]. Therefore, the evaluation strategy indicates a good performance and fitness of the calibrated benchmark model.

Emission Factors $\xi_{is}(t)$. — As it is assumed that information about climate change and its impacts is not disclosed to anyone in the benchmark model, the general equilibrium results over time have already been solved with all determined economic parameters previously. The results include a time series of the

[22]For visual comparison, please refer to Fig. A6 in the our online appendix.

real output ($Y_{is}(t)$). We then calculate the carbon emission factor data as the real CO_2 emission data divided by $Y_{is}(t)$ predicted by the benchmark model, denoted as $\hat{\xi}_{is}(t)$. The calibration of the carbon emission factor parameters $\xi_{is}(t)$ is supposed to make the carbon emission factors predicted by the model close to the real observations ($\hat{\xi}_{is}(t)$). As the emission factors are assumed to decrease and converge over time consistently, we parameterize the relative emission factors using the logistic growth model in equation III.7 with $t = 0$ representing the baseline year 2012.

$$N_{is}(t) \triangleq \frac{\xi_{is}(t)}{\xi_{is}(0)} \triangleq 1 - P_{\xi}^{is} + \frac{K_{\xi}^{is} P_{\xi}^{is}}{P_{\xi}^{is} + (K_{\xi}^{is} - P_{\xi}^{is}) e^{r_{\xi}^{is} t}} \tag{III.7}$$

At the baseline year 2012, the emission factors $\xi_{is}(0)$ should constitute point-to-point matches between the model predictions and the real emission data, i.e., $N_{is}(0) = 1$. The parameters $1 - P_{\xi}^{is}$ control the ultimately convergent level of emission factors. They are determined according to the benchmark projection (SSP5-8.5) in the IPCCAR6 where there is no policy intervention. The report predicts roughly $125Gt$ global CO_2 emissions in the next century, which is 3.574 times the global emission in 2012 (around $34.97Gt$). Given that the TFPs ($A_{is}(t)$) are convergent and fixed when $t \geq ssT$, the outputs $Y_{is}(t)$ are fixed at Y_{is}^* when $t \geq ssT$. Thus, the parameters $\bar{P}_{\xi}^{is}$ equal 3.574 times the relative values between $Y_{is}(0)$ and Y_{is}^* (see equation III.8).

$$1 - P_{\xi}^{is} = 3.574 \cdot \frac{Y_{is}(0)}{Y_{is}^*} \tag{III.8}$$

We determine the parameters remaining to generate the least square differences between $\hat{\xi_{is}}(t)$ and $\xi_{is}(t)$ from year 2001 to 2019. Table III.5 presents the calibration results[23]. Define the convergent status for the carbon emissions as $\frac{1}{N_{is}(t) - 1 + P_{\xi}^{is}} \frac{d(N_{is}(t) - 1 + P_{\xi}^{is}}{dt} < 0.1$ percent. The results indicate that the emission factors of the four sectors start to converge at $t = 27$, 28, 22, and 13, respectively. The calibration results show good fitness[24] between N_{is} and the targets from 2001 to 2019.

[23] Although the database covers the time span from 1997 to 2019, the data before 2001 is regarded as outliers because of the S-shape assumption of $\xi_{is}(t)$, especially for the sectors in the region B.

[24] See Fig A7 in the online appendix for the comparison

Table III.5—: The calibration results of emission factor parameters (equation III.7)

Sector is	r_ξ^{is}	P_ξ^{is}	K_ξ^{is}
Ah	0.197	0.852	1.672
Al	0.182	0.706	1.620
Bh	0.350	0.718	0.830
Bl	0.701	0.494	0.546

a AND *b*. — The parameters a and b control the power relation between temperature increase and atmospheric CO_2 concentration (equation II.10). The calibration is supposed to minimize the least square between the model and real data regarding temperature increases. We collect the global average atmospheric CO_2 record (1750 to 2020) from the Scripps CO_2 Program at the Scripps Institution of Oceanography at the University of California in San Diego[25] (Keeling et al., 2013). Because the record is not reported yearly, a linear interpolation technique is applied to the database to obtain yearly atmospheric CO_2 concentration in parts per million (ppm)[26]. In the meanwhile, NASA reports yearly land-ocean temperature index from 1880 to 2021 (GISTEMP, 2022). With the average land-ocean temperature index prior to 1990 defined as the pre-industrial level ($-0.219°C$), the temperature increases are obtained as the land-ocean temperature indexes above the pre-industrial level [27]. The calibration results are that $a = 3.427$ and $b = 1.387$. And the performance of the calibrated equation II.10 is presented in Fig. III.2.

D, $\bar{Q}$ AND λ. — To determine the value of D, it is essential to conjecture and justify the temperature increase which causes disastrous outcomes. The Intergovernmental Panel on Climate Change (IPCC) takes international responsibility for assessing the science related to climate change. In the IPCC AR5, the Representative Concentration Pathway with $8.5W/m^2$ (RCP8.5) corresponds with various undesirable catastrophes. In the latest sixth IPCC report, different Shared Socioeconomic Pathways (SSP1-5) are utilized to make predictions under different scenarios. According to the report, scenario SSP5-8.5 represents

[25] Atmospheric CO_2 record based on ice core data before 1958 (Etheridge et al., 1998; Macfarling Meure et al., 2006), and yearly averages of direct observations from Mauna Loa and the South Pole after and including 1958 from Scripps CO_2 Program.

[26] Fig. A8 in the online appendix shows the raw data and the linear interpolation, where the pre-industrial level is considered 280 ppm.

[27] The original data visualization is in Fig. A9 in the online appendix.

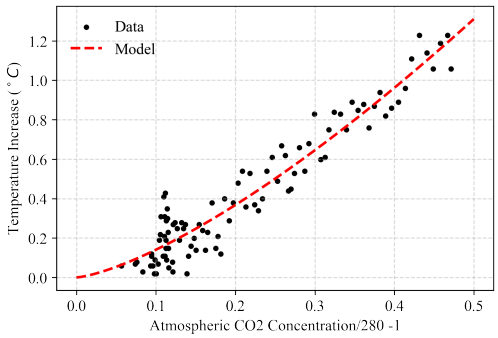

Figure III.2. : The power relation between atmospheric CO_2 concentration and temperature increases

Note: The line represents the calibrated result for the relationship in equation II.10.

the benchmark model without any policy interventions and bears an expected temperature increase of $4.4°C$ at the end of the century (with the medium confidence interval between $3.3°C$ to $5.7°C$). From the economics perspective, Stern and Stern (2007) believes a temperature increase of more than $5°C$ leads to the melting of the Greenland Ice Sheet and significantly raises the sea level by $7m$. Acemoglu et al. (2012) chooses the dangerous temperature as $6°C$ with the concern of sea level rises. Therefore, as the parameter D describes the totally unacceptable temperature increase such that economic activities mean nothing to people, we prefer $D = 7$ with high confidence to justify its disastrous characteristic from multiple sources. And we can obtain the corresponding dangerous atmospheric CO_2 concentration as $\bar{Q} = 748.6$, which reasonably characterizes the CO_2 concentration due to the temperature increase by $7°C$ according to the fifth report.

As the formulation of climate change impacts on households' aggregate consumption (equation II.8) is brought from Acemoglu et al. (2012), the calibration strategy for λ closely and carefully follows their practice. Like the DICE model, many other models introduce the impacts of climate change as a damage function to the total products. However, the climate change impacts here serve as a discount on households' aggregate consumption. To highlight similarities and differences quantitatively, the calibration should generate the climate change impacts $\psi(\Delta)$ close to the output losses in the previous models. Therefore[28], we find $\lambda = 0.4255$ to minimize the sum square of differences between the climate

[28]Fig. A10 in the online appendix presents the pattern of the function curve.

change discount factor and the effects of temperature rise in the DICE model[29] with the temperature increase up to $2.5°C$.

δ_i, G_i, κ_i AND Q_{i0}. — These parameters control the heterogeneous law of motion for the state variable Q_{it+1}, characterizing the vulnerability of climate change to regional carbon emissions. The calibration needs two variables for each region: the regional atmospheric CO_2 concentration Q_{it} and the regional carbon missions E_{it}. While the emission data is easy to acquire, we need to collect the atmospheric CO_2 concentration data at a more disaggregate level for the purpose of more reliable calibration for the heterogeneous law of motion for Q_{it+1} (equation II.A).

However, obtaining accurate and representative carbon concentration data for regions with large territories is a challenging task, as atmospheric CO_2 concentration is physically detected and measured in atmosphere background stations. The China Meteorological Administration (CMA) provides monthly observations of carbon concentration in seven atmosphere background stations in China, while the World Meteorological Organization (WMO) collects and releases atmospheric CO_2 concentration data from various background stations around the world. To construct a regional atmospheric carbon concentration data set that is both representative and longitudinal as much as possible, we combine the CMA and WMO data based on the locations of sites and the length of observations[30].

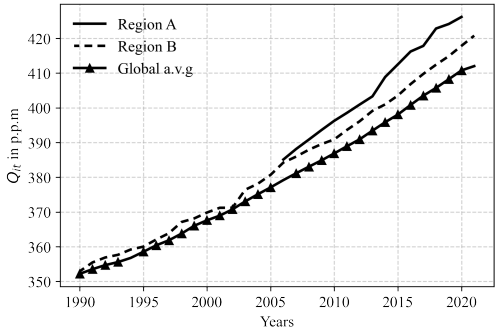

Figure III.3. : Constructed data set: Q_{At} and Q_{Bt}

Conclusively, the final results are summarized in Fig. III.3 with a comparison

[29]In the 2007's calibration of the DICE model (Nordhaus, 2007*a*), the damage function in terms of temperature rise equals $\frac{1}{1+0.005328\Delta^2}$ is estimated around $2.5°C$ and specifically for China.

[30]In addition to the CMA and the WMO, we sincerely acknowledge the Hong Kong Observatory and the World Data Centre forGreenhouse Gases (WDCGG) for data contribution. For details, please refer to our online appendix.

to the global average atmospheric CO_2 concentration. It is clear that both regions have higher carbon concentrations than the global average, and region A has a higher concentration pattern than region B, especially in recent decades. As for the initial state variables Q_{i0}, they have easily acquired as the regional atmospheric CO_2 concentration levels at the benchmark year 2012.

With the data of E_{it} and Q_{it} available, the calibration is easily accomplished. Given the value of δ_i, it is straightforward to determine the parameters G_i and κ_i using the OLS regression in equation III.9 rewritten from the law of motion for the state variable Q_{it+1}.

$$\text{(III.9)} \quad \ln[(Q_{it+1} - 280) - (1 - \delta_i)(Q_{it} - 280)] = \ln G_i + \kappa \ln E_{it} + \text{Error Term}$$

And then, we can obtain the model predictions of $\hat{Q}_{it}$ using the law of motion with the year 2012 as the dynamic motion starting point. The selection of δ_i is aimed to generate the least square differences between $\hat{Q}_{it}$ and real data Q_{it}. And the calibration results are summarized in Table III.6. The calibrated law of motion exhibits very similar patterns of Q_{it} between the model predictions and the real data[31].

Table III.6—: The calibration results of the law of motion for the state variable Q_{it+1}

Region i	δ_i	G_i	κ_i	Q_{i0}
A	0.0430	5.691***	0.4722*	400.9
B	0.0433	4.015***	0.3361***	396.1

Note: The parameters G_i and κ_i are coefficients of the OLS regression in equation III.9.

*** Significant at the 1 percent level.

** Significant at the 5 percent level.

* Significant at the 10 percent level.

Summary of Calibration Results. — In summary, all parameters are determined such that the model exhibits the best prediction to observed data. The calibration results and relevant information are concluded in Table III.7 below.

[31] To visually compare the fitness, see Fig. A11 in the online appendix

Table III.7—: Summary of the Calibration Results

Parameter	Reference	Result
$A_{is}(0)$	Eq. II.1	Table III.3
$g_s(0)$ and δ_A	Eq. III.5	$g_h(0) = 0.036, g_l(0) = 0.026, \delta_A = 0.035$
K_L, P_L, r_L	Eq. III.1	Table III.2
K_L^A, P_L^A, r_L^A	Eq. III.2)	Table III.2
α_{is}^m	Eq. II.1	Table III.1
σ, ω_{is}^{jm}	Eq. II.2	$\sigma = 3$, ω_{is}^{jm} in Table III.3
ϵ, η_i^{jm}	Eq. II.5	$\epsilon = 3$, Table III.3
ρ	Eq. II.3	0.98
$\beta, \gamma_h, \gamma_l$	Eq. II.4	$\beta = 0.0527, \gamma_h = 0.557, \gamma_l = 0.443$
a, b	Eq. II.10	$a = 3.427, b = 1.387$
λ, D	Eq. II.8	$\lambda = 0.4255, D = 7$
$\bar{Q}$	$\triangleq 280[(\frac{D}{a})^{\frac{1}{b}} + 1]$	748.6
$Q_{i0}, \delta_i, G_i, \kappa_i$	Eq. II.A	Table III.6
$K_\xi^{is}, r_\xi^{is}, P_\xi^{is}$	Eq. III.7	Table III.5

IV. Quantitative Results and Implications

Given the scrutinized calibration in the previous section, the calibrated benchmark model exhibits exceptional performance in mapping the model variables to real observations. In this section, we explore the quantitative results of the benchmark and social planner models, highlight some policy implications through comparison, and provide quantitative predictions of the economy. By their name, scenario (1) represents the results of the benchmark model, i.e., the "laissez-faire" economy, and scenario (2) refers to the results of the social planner model, i.e., the introduction of a social planner with Pareto efficiency[32].

Before any discussions, we need to clarify how the numerical results are obtained. Firstly, all time-variant exogenous variables change, converge to certain levels until period $ssT = 100$ and become fixed afterward. Secondly, we find the unique steady state for each model. Thirdly, both backward shooting (BWS) and forward shooting (FWS) methods are adopted to find the dynamic results of the equilibrium path. The FWS stops at the period when all variables are within the 0.5% range to their steady-state levels, denoted as Tss. And the system jumps to the steady state at the next period $(Tss + 1)$ and remains the same status for infinite time remaining. Table IV.1 provides this information.

[32] A social planner can always achieve Pareto improvement beyond the benchmark model by choosing a proper weight, e.g., $\theta = 0.63727322$ in our analysis.

Table IV.1—: Basic information about the numerical methods for dynamic results

Scenario	Q_{A0}	Q_{B0}	Tss	Q_{ATss}	Q_{BTss}	Q_A^*	Q_B^*
(1)	400.938	396.125	150	633.270	557.934	636.366	559.382
(2)	400.925	396.120	138	562.445	548.901	563.628	550.859

A. *The Social Planner Optimal Path*

Details of Policy Implications. — In scenario (2), the social planner model with Pareto efficiency suggests proportional tax rates and lump-sum rebate rates by regions to achieve the optimal path. According to equation II.18, the tax rates are determined based on the difference between shadow prices and carbon-deducted shadow prices of products, i.e., $(1 - \frac{\tilde{\lambda}_{is}(t)}{\lambda_{is}(t)})$. The composition and usage of taxes collected by the central government are illustrated in equation II.20, which indicates how to rebate to households. This equation does not indicate about the relationship between the amount of rebates and taxes within a region. It is possible that one region contributes more taxes than the rebates to its households. In addition, it does not guarantee that the rebate is positive, although the tax rates are definitely positive as $\tilde{\lambda}_{is}(t) < \lambda_{is}(t)$. The negative rebates mean that the central government should take away some incomes from the households. Indeed, the scenario (2) suggests lump-sum taxes (negative rebates) on the people in region A at the first several periods (Fig. IV.2).

The time patterns of the tax rates on production sectors implied by scenario (2) are displayed in Fig. IV.1. The tax rates increase over time as the concentration of atmospheric CO_2 accumulates and the social costs of emissions become greater. It is evident that the social central planner model suggests higher tax rates for sector Ah and lower tax rates for sector Bh. It implies that the social costs of carbon emissions are greater and the value of better climate conditions is larger in region A. The tax rates for the low-emission sectors are very minor, ranging from $0.11\% - 0.9\%$ on sector Al and ranging $0.08\% - 0.54\%$ on sector Bl.

To align with carbon taxes (CNY per ton CO_2) as a common practice, we adopt the prices in the baseline year 2012 as the fixed price level[33]. Table IV.2

[33]For international comparison, the exchange rate between CNY and USD was around 6.3CNY/USD in 2012.

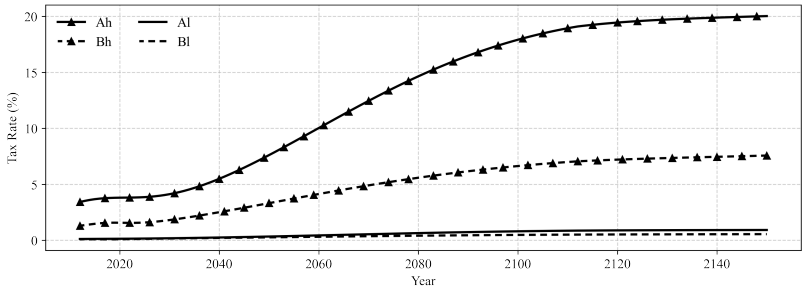

Figure IV.1. : Proportional tax rates implied by the social planner

summary the implied carbon taxes by sectors and the national average in some years[34]. The carbon taxes for the four sectors Ah, Al, Bh and Bl increase by 2.7%, 2.4%, 2.2%, and 1.9% yearly on average, respectively, as larger Q_{it} and aggregate consumption lead to more significant social costs of carbon emissions. We can also obtain that the national average real carbon cost was 64CNY/tCO_2 in 2012 and grows by 2.3% yearly on average (at 2012 fixed price level). Although such carbon taxes are higher than most existing practices(World Bank, 2021), it is still lower than the level required to achieve the Paris Agreement[35].

Table IV.2—: Carbon taxes implied by scenario (2) in 2012 *yuan* CNY per ton CO_2

Sector	2012	2020	2030	2100	2150
Ah	152	382	934	5398	6036
Al	159	343	729	3806	4363
Bh	38	90	182	692	790
Bl	39	79	141	427	490
National a.v.g.	64	153	314	1394	1552

In addition to the tax rates, which explains how the tax is collected, the expenses of tax revenue is crucial to fully implement the policy. Fig. IV.2 shows the structure of taxation and rebates between the two regions from the perspective of central government. As implied by equation II.20, the rebates received by one region do not have to equal the taxes paid. Quantitatively, the results show that region A contributes more taxes than the rebates at first (even with negative rebates, or equivalently lump-sum taxes from households), and gradually received more rebates than tax payment later on.

Economic policies are crucial to reduce carbon emissions and cope with the

[34]Fig. A12 in the online appendix shows the detailed patterns of carbon taxes.
[35]Using GDP deflator and exchange rate in 2020, we suggest a carbon cost at 22USD/tCO_2 in 2020 current price, but the advice of Paris Agreement is 40-80 USD/tCO_2

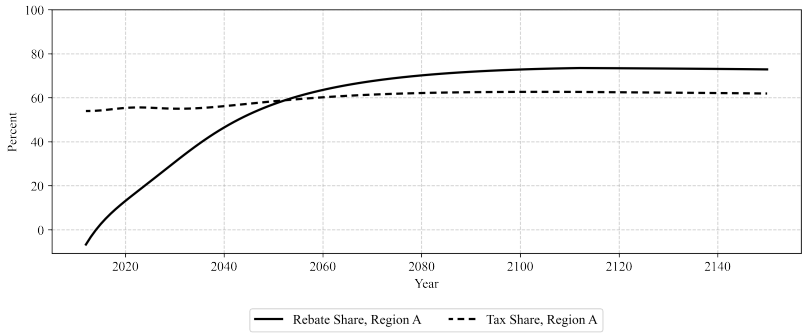

Figure IV.2. : Share of Rebates to and Taxes from region A

Note: According to the notations in equation II.20, the share of rebates to region A is calculated as $\frac{rebate\ to\ region\ A}{rebate\ to\ region\ A + rebate\ to\ region\ B}$ and the share of taxes from region A is calculated as $\frac{tax\ revenue\ from\ region\ A}{tax\ revenue\ from\ region\ A + tax\ revenue\ from\ region\ B}$.

risk of climate change. As one of the most effective and equitable methods, carbon taxes are indeed implemented in real world, especially countries with low emissions. The literature on carbon taxes has extensively discussed various aspects such as the optimal tax rates, implementation challenges, and other related issues[36]. This study justifies the feasibility of industry-specified proportional taxes and regional lump-sum rebates through the market equilibrium mechanism. Moreover, the study reveals quantitative details and consequences of implementing these policies, which may interest policymakers.

Emissions and Climate Change. — We analyze the patterns of regional carbon emissions and temperature rise above the pre-industrial era. Fig. IV.3 illustrates a comparative analysis of regional carbon emissions under the two scenarios, which includes the model projection of regional carbon emissions and the real data (2001 to 2019). The findings of our study reveal strikingly similar temporal patterns of emissions across different regions, characterized by (i) a temporal decline at the early stage in emissions due to substantial and rapid decreases in emission factors $\xi_{is}(t)$; (ii) a subsequent steady rise in emissions, wherein the decline of emission factors slows down while output productivity continues to increase; and (iii) emissions eventually reaching a plateau as all relevant parameters attain a stable state beyond the threshold of $t \geq ssT$. Notably, scenario (2) demonstrates an ability to consistently reduce carbon emissions over time compared to scenario (1). Compared to scenario (1), scenario (2)

[36]For details, please see a literature review by Timilsina (2022).

exhibits a minor reduction in regional carbon emissions during the early stages, and the reduction is gradually deepened to approximately 38.7% for region A and roughly 8.5% for region B later on. At the national level, carbon emissions are initially reduced by 0.3 G.t (3.2%). This reduction consistently expands as time progresses, reaching an estimated value of approximately 5.4 G.t (15.5%) by the middle of the next century.

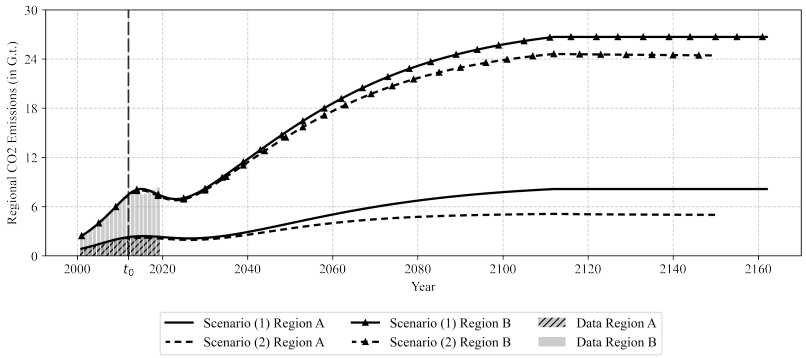

Figure IV.3. : Projection of regional carbon emissions

Based on the projection of emission patterns, we shed light on the ongoing debate about the Chinese carbon peak. Although the Chinese government has committed to achieving carbon peak by 2030, there is no consensus on when the peak will occur. According to the study by Mi et al. (2017), the peak could occur before 2030 with solid policy interventions, while it could be delayed given the ambitious commitment and uncertainty risks (Qi et al., 2020). However, the results of this study focus on optimal balance between climate mitigation and social welfare, other than the feasibility of Chinese carbon peak. And the predictions are based on the assumption that there are no further interventions or out-of-trend innovations. The differences between the social planner scenarios (2) and the benchmark scenario (1) only show quantitatively how much the implied policies can cut emissions through the market's general equilibrium. Therefore, based on the results, we can only say that, besides the implied tax-and-rebate policies, higher intensity and larger scale interventions, such as low-carbon technology breakthroughs, are needed to achieve the Chinese carbon peak.

Based on the results presented in Table IV.1, the policy interventions implied

by the social planner can help mitigate the atmospheric CO_2 concentration and curb the problem of climate change, particularly in region A. As shown in Table IV.3, the temperature increases across various time stages are lower in scenarios (2) compared to the benchmark scenario (1), especially for region A at later stages. These findings demonstrate the feasibility and effectiveness of the tax-and-rebate policy interventions proposed in this study. Specifically, the temperature rise would decline by around $1.3°C$ in region A and slightly by $0.2°C$ in region B in the middle of the next century. The predictions are similar to Nordaus's RICE/DICE results that the optimal temperature rise is around $3°C$ in the next century (Nordhaus, 2011; Nordhaus and Yang, 1996). However, it is essential to note that the projected temperature increases are far from the IPCC's advocates of limiting global warming to $1.5°C$ in the coming century. Therefore, additional interventions will be necessary for more significant climate change mitigation.

Table IV.3—: Temperature rises above the pre-industrial level at various time stages ($°C$)

Region	Scenario	2012	2050	2100	Steady State
A	(1)	1.070	2.104	3.978	4.788
	(2)	1.070	1.962	3.178	3.476
B	(1)	1.011	1.977	3.057	3.417
	(2)	1.011	1.952	2.967	3.280

Note: The temperature rises in the year 2150 are very close to the "Steady State" levels.

Welfare: Equivalent Constant Aggregate Consumption. — The summation of discounted utility with an infinite time horizon, denoted as $\mathbf{V}_i$, is an important ordinal measurement of regional welfare. The numerical calculation is presented in equation IV.1 where U_i^* represents the utility at the steady state.

$$\mathbf{V}_i = \sum_{t=0}^{T} \left(\rho^t L_{it} U_{it}\right) + \frac{\rho^{T+1} L_{iT} U_i^*}{1-\rho} \tag{IV.1}$$

By comparing the sizes of $\mathbf{V}_i$ between different models, we can conclude whether households in the region i get better off or worse off. However, restricted by the ordinal measurement $\mathbf{V}_i$, we can not naively interpret the intervals or compare $\mathbf{V}_A$ and $\mathbf{V}_B$. Based on the fact that μ_{it} measures the aggregate consumption as the number of joint baskets in 1990 composition, the intervals between μ_{it}

are interpreted as more (or less) baskets consumed. And $\Phi_{it}\mu_{it}$ means the number of baskets consumed discounted by the climate change impacts in a sense that one basket with the climate change impacts $\Phi_{it} < 1$ is equivalent to Φ_{it} unit basket with pleasant climate situation in pre-industrial era. Therefore, we can create an equivalent constant aggregate consumption with an infinite time horizon, denoted as $\bar{\mu}_i$ in equation IV.2, to compare welfare across regions and scenarios reasonably. Moreover, $\bar{\mu}_i$ is a ratio measurement for $\mathbf{V}_i$, interpreted as "the number of joint baskets consumed by households under pleasant climate conditions ($\Phi_{it} = 1$)".

$$\mathbf{V}_i = \ln \bar{\mu}_i \big[\sum_{t=0}^{T} \rho^t L_{it} + \frac{\rho^{T+1}}{1-\rho} L_{iT} \big] \tag{IV.2}$$

Table IV.4 displays the outcomes of aggregation of the present values of utility ($\mathbf{V}_i$) and the equivalent constant aggregate consumption ($\bar{\mu}_i$). Scenario (2) constitutes Pareto efficiency because the social planner efficiently deals with the externality of carbon emissions. Specifically, the equivalent constant consumption increases by 1.2% for region A and slightly by 0.2% for region B. The magnitude of increase is substantial, although the percentage seems small. For instance, the 1.2% increase in $\bar{\mu}_A$ means that the households experience such an increase in utility flow for each period forever as if the climate condition is pleasant. The improvement in people's welfare justifies the policy implications because (1) the improvement stems exclusively from fiscal policies since all productivity-relevant parameters remain unchanged, and (2) the climate conditions are significantly protected in addition to the increase in people's welfare. Furthermore, the comparison between $\bar{\mu}_A$ and $\bar{\mu}_B$ suggests that every household in the advanced region A enjoys roughly 45 more joint consumption baskets than the backward region B due to their higher incomes. This inter-regional comparison would not be feasible without the equivalent constant aggregate consumption.

Table IV.4—: Regional welfare comparisons

	Scenario (1)	Scenario (2)	% Change
$\bar{\mu_A}$	101.83	103.04	1.19
$\bar{\mu_B}$	58.37	58.53	0.27

Scenario (2) findings originate from the social planner model that utilizes a

specific weight θ to attain Pareto efficiency. Varying degrees of θ produce distinct sets of $(\bar{\mu}_A, \bar{\mu}_B)$ pairs, which establish the possibility frontier of $\bar{\mu}_i$. This frontier encompasses all outcomes of $(\bar{\mu}_A, \bar{\mu}_B)$ that the central planner can execute. Figure IV.4 illustrates this possibility frontier of regional equivalent constant aggregate consumption. Since the results of scenario (1) are already near the possibility frontier, scenario (2) yields only a minor Pareto improvement.

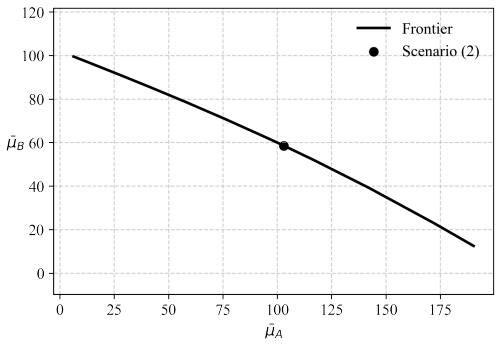

Figure IV.4. : Possibility frontier of regional equivalent constant aggregate consumption $\bar{\mu}_i$

Production and Real Value Added. — To compare the value added across different scenarios and periods, we use the fixed prices of the baseline year 2012 to calculate the real national GDP or real value added at different levels for both scenarios[37]. Since the time patterns are very similar for each sector across scenarios (i.e., increasing, concave, and convergent) a table summary is enough to present the results. Table IV.5 shows the results and comparison. According to the calibrated benchmark model, the average growth rate of real value added between 2012 and 2100 for the four sectors are 4.2%, 2.5%, 3.4%, and 1.9%, respectively. The national average growth rate is 2.5%, with 2.8% for region A and 2.3% for region B. As the calibration assumes the convergence of total factor productivity, we observe conservative growth regarding real value added or real GDP.

By comparing the percent changes between scenario (2) and scenario (1), we can discover the effects of the tax-and-rebate policies or the introduction of a social planner. At the national level, real GDP declines slightly by less than one

[37]Fig. A13 in the online appendix shows the detailed diagrams of the real value added by sectors for different scenarios.

percent. At the regional level, region A loses real value added while region B gains real value added in both scenarios. At the sector level, the real value added of the high-emission sectors drops sharply, and that of the low-emission sectors rises significantly. It implies that reducing carbon emissions requires reducing output, but not necessarily value-added, which equals output minus intermediate input.

Table IV.5—: Real value added and comparison between two scenarios

	Total		High-emission sector		Low-emission sector	
Time Stages	(1)	(2)-(1)	(1)	(2)-(1)	(1)	(2)-(1)
			The Nation			
2012	54.1	−0.03%	14.3	−2.80%	93.9	0.39%
2050	297.3	−0.24%	180.0	−8.08%	414.5	3.17%
2100	484.9	−1.11%	356.9	−18.59%	612.9	9.07%
Steady State	501.7	−1.37%	374.2	−20.83%	629.2	10.20%
			Region A			
2012	21.0	−0.06%	2.3	−6.16%	18.7	0.69%
2050	141.9	−0.75%	39.0	−14.75%	102.9	4.56%
2100	247.5	−3.22%	84.6	−34.31%	162.9	12.92%
Steady State	257.3	−3.80%	89.2	−37.98%	168.1	14.35%
			Region B			
2012	33.1	−0.01%	4.8	−1.20%	28.3	0.19%
2050	155.4	0.24%	50.9	−2.97%	104.4	1.80%
2100	237.4	1.10%	93.9	−4.42%	143.6	4.71%
Steady State	244.4	1.18%	97.9	−5.20%	146.5	5.44%

Note: Columns "(1)" shows the real value added of the "laissez-faire" scenario in 2012 trillion CNY, and column "(2)-(1)" computes the relative changes in real value added between scenarios (2) and scenario (1). All prices take the fixed prices of the four differentiated products at $t = 0$ (year 2012).

Our findings contribute to the existing discussion on the relationship between economic returns and carbon emissions. While reduction in carbon emission is possibly associated with lower economic growth (Heil and Selden, 2001), there is no clear causal link between them (Zhang and Cheng, 2009), and the literature on the causal relationship is ambiguous and controversial (Huang, Hwang and Yang, 2008). Our findings show that a 1.5 percent decrease in real GDP at the national level leads to a 15% decrease in carbon emissions in the middle of the next century. However, in the meanwhile, this relationship does not hold for two regions within the country: region A experiences a 3.8% drop in real value added and a significant reduction in carbon emissions. In contrast, region B sees a 1.2% increase in real value added and a noticeable reduction in carbon

emissions. These contrasting outcomes indicate that cuts in carbon emissions and economic development are not necessarily correlated.

Interestingly, both regions cut down emissions but experience opposite changes in real value added. The regional differences in income level and climate sensitivity can explain the situation. In our model, region A has a higher income per capita and is more vulnerable to climate change than region B, which implies a higher social cost of carbon emissions for region A. This motivates region A to take more drastic measures to reduce carbon emissions, such as cutting down the production of high-emission sectors and outsourcing more products from region B. These two factors lead to lower real value added for region A and higher real value added for region B.

Emissions embodied in uses v.s. direct emission. — In this model, carbon emissions are directly generated from the production process and affect the climate where the sectors are located. However, products only partially benefit the local economy as intermediates or consumption due to the inter-region trades. The emissions generated in one region may not equal the emissions embodied in the products used by the region, whether intermediates or consumption. We name the former emissions direct emissions and the latter embodied in uses. Fig. IV.5 exhibits the differences between two types of emissions of region A under the two scenarios, i.e., the emissions embodied in uses minus the direct emission. The emissions embodied in the uses of products are larger than its direct

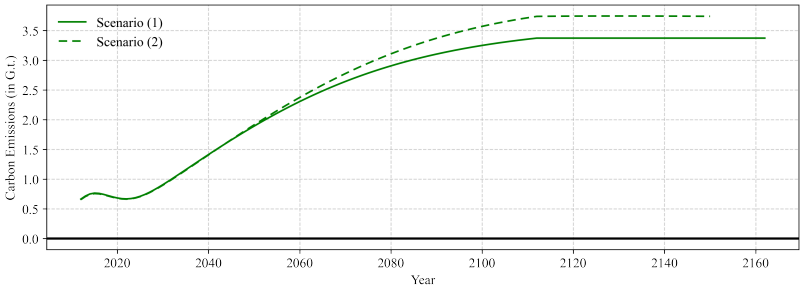

Figure IV.5. : Region A: emissions embodied in uses - direct emissions

emissions, which means region A outsources its emissions to region B. Compared to the benchmark scenario (1), region A outsources even more in scenario (2). This tells that the social planner is willing to allocate more emissions to region B when balancing climate change and economic development and pursuing Pareto

improvement. The social planner proposes this distribution because it is indeed beneficial to both regions: region A improves the climate conditions by outsourcing CO_2 as its climate is much more vulnerable to carbon emissions than the other region; the under-developed region B gains extra income through the trade given its relatively stable climate. Such a pattern that the developed provinces outsource CO_2 to the less-developed in-land provinces is also documented by Feng et al. (2013). While they regard the pattern as inequity to some extent, we consider it a way of improving social welfare.

B. Adherence to the Paris Agreement

The Paris Agreement, adopted in December 2015, is a landmark international treaty under the United Nations Framework Convention on Climate Change (UNFCCC). Its primary objective is to combat climate change by limiting global warming to well below 2 degrees Celsius above pre-industrial levels. As the largest CO_2 emitter, China ratified the Paris Agreement in 2016 and made its commitment of carbon peak by 2030 which is a crucial step towards achieving the long-term goal of $2°C$ temperature rise limit. However, according to results of scenario (2), the temperature rise restriction of $2°C$ do not align with the optimal welfare path in the two regions. The potential cost of achieving the Paris Agreement goal remains ambiguous and valuable to policy makers. Therefore, it becomes crucial to assess the potential impacts of Chinese adherence to $2°C$ limit. We investigate the optimal path for the scenario in which the social planner additionally faces the temperature rise constraints of both regions, denoted as scenario (3), while the regional welfare weight θ remains as previously[38].

Fig IV.6 exhibits the patterns of several important variables of scenarios (2) and (3), including temperature rises, carbon emissions, real value added, and the utility flow ($L_{it}U_{it}$) for both regions. According to the results, temperature rises are limited to the $2°C$ goal of the Paris Agreement since the year 2066 and 2065 for region A and B respectively. In scenario (3), carbon emissions exhibit consistent declines around the year 2050 as temperature rises approach the limit. By the middle of next century, the national carbon emissions are greatly reduced

[38]For details of equations, please refer to B.B3 in our online appendix.

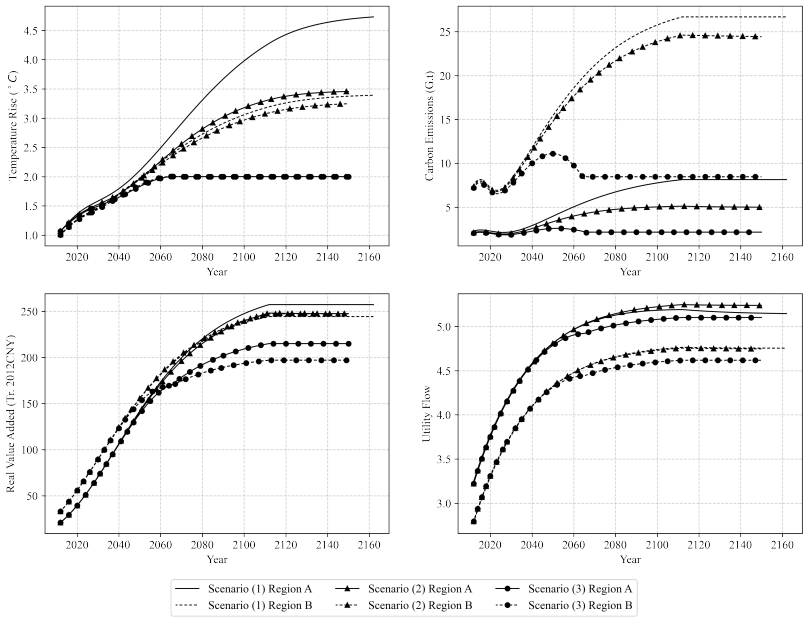

Figure IV.6. : Comparisons of some variables among scenarios

by around 64% and limited to 10.6 G.t which is offset by the regional natural carbon absorption. In the year 2150, however, sticking to the Paris Agreement goal leads to almost 14% losses in real regional value added to region A and 30% to region B, compared to socially optimal path in scenario (2). At the national scale, the substantial losses in the two regions cause the GDP declines by around 17%. In terms of welfare, the losses in utility flows mainly occur in future periods. And the equivalent constant aggregate consumption $\bar{\mu}_i$ are 97.01 for region A and 55.87 for region B in scenario (3). Compared to the results in Table IV.4, this represents declines for each region by 5.8% and 4.5% from scenario (2), and by 4.7% and 4.3% from the benchmark scenario (1), respectively.

Losses in economic development and welfare between scenarios (2) and (3) highlight uncertain risks of sticking to the $2°C$ temperature rise limit goal in the Paris Agreement. The model assumes no out-of-trend technology breakthroughs, so prioritizing and investing in low-carbon technologies can decouple carbon emissions from economic activities and alleviate adverse effects of climate change. This research emphasizes the importance of innovation and technological advancements in pursuing the $2°C$ goal without compromising economic growth and welfare.

V. Conclusion

In conclusion, this study tackles balancing economic growth and climate change in China using a multi-region and multi-sector model with climate change. Calibrated with real-world data and IPCC projections, the model performs well in fitting observations and explores various scenarios for optimal paths and policy implications. Results are based on conservative assumptions, excluding potential technological breakthroughs in carbon emission technology.

The benchmark scenario shows a temperature rise of $4.7°C$ and $3.7°C$in regions A and B, respectively, by mid-century if no action is taken. Implementing carbon taxes and household rebates can balance economic development and climate change, reducing temperature rise in region A by about $1°C$, but the national GDP is projected to decline by around 1.4%.Persisting in achieving the Paris Agreement's objective results in consistent losses in welfare of approximately 5.8% and 4.5% for both regions, and the real national GDP is projected to decline by around 17% in the middle of the next century, highlighting the significant trade-offs and challenges associated with balancing environmental sustainability and economic growth.

In summary, this research provides valuable insights into the optimal path for balancing China's economic development and climate change. By considering different scenarios and implementing policies that combine carbon taxes and household rebates, it is possible to mitigate the long-term temperature rise and achieve a more sustainable future. However, it is crucial to acknowledge the limitations of the research, particularly regarding conservative assumptions about technological advancements that could significantly influence the results. Future breakthroughs and advancements in carbon emission technology should be continuously monitored and integrated into the analysis to refine further and enhance the findings of this research.

Lastly, achieving the Paris Agreement goals requires technology development in climate change mitigation. Relying solely on market equilibrium distribution of resources can only limit the temperature rise to about 3.3 degrees Celsius. Proactive technology development is needed, including research investment, international collaboration, and clean technology adoption. Further studies focus-

ing on R&D strategies and their implications for climate change mitigation are valuable to complement this research's findings.

REFERENCES

Acemoglu, Daron, Philippe Aghion, Leonardo Bursztyn, and David Hemous. 2012. "The environment and directed technical change." *American economic review*, 102(1): 131–66.

Brandt, Loren, and Carsten A. Holz. 2006. "Spatial Price Differences in China: Estimates and Implications." *Economic Development and Cultural Change*, 55(1): 43–86.

Broda, Christian, and David E Weinstein. 2006. "Globalization and the Gains From Variety." *The Quarterly journal of economics*, 121(2): 541–585.

Calel, Raphael, Jonathan Colmer, Antoine Dechezleprêtre, and Matthieu Glachant. 2021. "Do carbon offsets offset carbon?"

Etheridge, DM, LP Steele, RL Langenfelds, RJ Francey, JM Barnola, and VI Morgan. 1998. "Historical CO2 records from the Law Dome DE08, DE08-2, and DSS ice cores." *Trends: a compendium of data on global change*, 351–364.

Feng, Kuishuang, Steven J Davis, Laixiang Sun, Xin Li, Dabo Guan, Weidong Liu, Zhu Liu, and Klaus Hubacek. 2013. "Outsourcing CO2 within china." *Proceedings of the National Academy of Sciences*, 110(28): 11654–11659.

Gao, Yuning, Meng Li, Jinjun Xue, and Yu Liu. 2020. "Evaluation of effectiveness of China's carbon emissions trading scheme in carbon mitigation." *Energy Economics*, 90: 104872.

GISTEMP, Team. 2022. "GISS Surface Temperature Analysis (GISTEMP), version 4." *NASA Goddard Institute for Space Studies*.

Guan, Dabo, Yuli Shan, Zhu Liu, and Kebin He. 2016. "Performance assessment and outlook of China's emission-trading scheme." *Engineering*, 2(4): 398–401.

Guan, Yuru, Yuli Shan, Qi Huang, Huilin Chen, Dan Wang, and Klaus Hubacek. 2021. "Assessment to China's recent emission pattern shifts." *Earth's Future*, 9(11): e2021EF002241.

Heil, Mark T, and Thomas M Selden. 2001. "Carbon emissions and economic development: future trajectories based on historical experience." *Environment and Development Economics*, 6(1): 63–83.

Huang, Bwo-Nung, Ming Jeng Hwang, and Chin Wei Yang. 2008. "Causal relationship between energy consumption and GDP growth revisited: a dynamic panel data approach." *Ecological economics*, 67(1): 41–54.

Huang, Yongfu, Terry Barker, et al. 2008. *The Clean Development Mechanism and sustainable development: a panel data analysis.* University of Cambridge, Environmental Economy and Policy Research Group.

Inklaar, Robert, and Marcel P. Timmer. 2014. "The Relative Price of Services." *Review of Income and Wealth*, 60(4): 727–746.

Keeling, RF, SC Piper, AF Bollenbacher, and SJ Walker. 2013. "Scripps CO2 program." *Dernière consultation*, 24.

Liu, Zhu, Zhu Deng, Gang He, Hailin Wang, Xian Zhang, Jiang Lin, Ye Qi, and Xi Liang. 2021. "Challenges and opportunities for carbon neutrality in China." *Nature Reviews Earth & Environment*, 1–15.

Lyu, Jing, Tianle Liu, Bofeng Cai, Ye Qi, and Xiaoling Zhang. 2023. "Heterogeneous effects of China's low-carbon city pilots policy." *Journal of Environmental Management*, 344: 118329.

Macfarling Meure, Cecelia, David Etheridge, Cathy Trudinger, P Steele, R Langenfelds, T Van Ommen, A Smith, and J Elkins. 2006. "Law Dome CO2, CH4 and N2O ice core records extended to 2000 years BP." *Geophysical Research Letters*, 33(14).

Mi, Zhifu, Yi-Ming Wei, Bing Wang, Jing Meng, Zhu Liu, Yuli Shan, Jingru Liu, and Dabo Guan. 2017. "Socioeconomic impact assessment of China's CO2 emissions peak prior to 2030." *Journal of cleaner production*, 142: 2227–2236.

Nordhaus, William. 2007*a*. "Accompanying Notes and Documentation on Development of DICE-2007 Model: Notes on DICE-2007. delta. v8 as of September 21, 2007." *Miscellaneous publication, Yale University, New Haven, NE.*

Nordhaus, William D. 1991. "To slow or not to slow: the economics of the greenhouse effect." *The economic journal*, 101(407): 920–937.

Nordhaus, William D. 1992*a*. "An optimal transition path for controlling greenhouse gases." *Science*, 258(5086): 1315–1319.

Nordhaus, William D. 1992*b*. "The 'Dice' Model: Background and Structure of a Dynamic Integrated Climate-Economy Model of the Economics of Global Warming." *Cowles Foundation Discussion Papers. 1252.*

Nordhaus, William D. 1994. *Managing the global commons: the economics of climate change.* Vol. 31, MIT press Cambridge, MA.

Nordhaus, William D. 2007*b*. "A review of the Stern review on the economics of climate change." *Journal of economic literature*, 45(3): 686–702.

Nordhaus, William D. 2011. "Estimates of the social cost of carbon: background and results from the RICE-2011 model." National Bureau of Economic Research.

Nordhaus, William D. 2017. "Revisiting the social cost of carbon." *Proceedings of the National Academy of Sciences*, 114(7): 1518–1523.

Nordhaus, William D, and Zili Yang. 1996. "A regional dynamic general-equilibrium model of alternative climate-change strategies." *The American Economic Review*, 741–765.

Paulsson, Emma. 2009. "A review of the CDM literature: from fine-tuning to critical scrutiny?" *International environmental agreements: politics, law and economics*, 9: 63–80.

Qi, Ye, Nicholas Stern, Jian-Kun He, Jia-Qi Lu, Tian-Le Liu, David King, and Tong Wu. 2020. "The policy-driven peak and reduction of China's carbon emissions." *Advances in Climate Change Research*, 11(2): 65–71.

Schneider, Lambert, and Anja Kollmuss. 2015. "Perverse effects of carbon markets on HFC-23 and SF6 abatement projects in Russia." *Nature Climate Change*, 5(12): 1061–1063.

Shan, Yuli, Dabo Guan, Heran Zheng, Jiamin Ou, Yuan Li, Jing Meng, Zhifu Mi, Zhu Liu, and Qiang Zhang. 2018. "China CO2 emission accounts 1997–2015." *Scientific data*, 5(1): 1–14.

Shan, Yuli, Jianghua Liu, Zhu Liu, Xinwanghao Xu, Shuai Shao, Peng Wang, and Dabo Guan. 2016. "New provincial CO2 emission inventories in China based on apparent energy consumption data and updated emission factors." *Applied Energy*, 184: 742–750.

Shan, Yuli, Qi Huang, Dabo Guan, and Klaus Hubacek. 2020. "China CO2 emission accounts 2016–2017." *Scientific data*, 7(1): 54.

Stern, Nicholas, and Nicholas Herbert Stern. 2007. *The economics of climate change: the Stern review.* cambridge University press.

Timilsina, Govinda R. 2022. "Carbon taxes." *Journal of Economic Literature*, 60(4): 1456–1502.

World Bank. 2021. *State and Trends of Carbon Pricing 2021.* Washington, DC:World Bank Publications.

Zhang, Xing-Ping, and Xiao-Mei Cheng. 2009. "Energy consumption, carbon emissions, and economic growth in China." *Ecological economics*, 68(10): 2706–2712.

Zheng, Heran, Zengkai Zhang, Wendong Wei, Malin Song, Erik Dietzenbacher, Xingyu Wang, Jing Meng, Yuli Shan, Jiamin Ou, and Dabo Guan. 2020. "Regional determinants of China's consumption-based emissions in the economic transition." *Environmental Research Letters*, 15(7): 074001.